MODELLING AND TESTING TECHNIQUES FOR GEARBOX ANALYSIS AND OPTIMIZATION

Angelo Oreste Andrisano
Department of Engineering "Enzo Ferrari",
University of Modena and Reggio Emilia, Italy
E-mail: angelooreste.andrisano@unimore.it

Francesco Pellicano
Department of Engineering "Enzo Ferrari",
University of Modena and Reggio Emilia, Italy
E-mail: francesco.pellicano@unimore.it

Marco Barbieri
Department of Engineering "Enzo Ferrari",
University of Modena and Reggio Emilia, Italy
E-mail: mark@unimore.it

Antonio Zippo
Department of Engineering "Enzo Ferrari",
University of Modena and Reggio Emilia, Italy
E-mail: antonio.zippo@unimore.it

Matteo Strozzi
Department of Engineering,
University of Ferrara, Italy
E-mail: strmtt@unife.it

Abstract*. In this paper pitting phenomenon and stress distribution of gears are investigated by means of experimental activities and numerical finite element analyses. In the first part, results of experimental accelerated endurance tests for the investigation of the pitting phenomenon of gears are reported. These durability tests are made at a specific nominal load and far from the resonance. After a short time, a visible pitting phenomenon arises. In the second part, finite element numerical analyses for the evaluation of gear stresses are given. The numerical analyses start from stress-vibration correlations and dynamic factors obtained by means of a 2-dof dynamic model previously developed; these results are used in the dynamic FEM simulations to calculate maximum normal stress and contact pressure on the contact tooth of the pinion vs. vibration amplitude for different dynamic factors.*

Keywords*: industrial gearboxes, pitting phenomenon, stress distribution*

1. INTRODUCTION

Pitting and stress analyses deeply improve the mechanical resistance of gear teeth, which are subjected to very high contact pressures and fatigue loads in operating conditions [1-5];

gear dynamic optimization and profile modification can increase gearbox reliability [6-8].

Moreover, the analysis of the effects of surface pitting and wear on the vibration of a gear transmission together with the investigation of pressure and normal stress distributions in gears can improve the mechanical properties of the mechanical system [9-10].

In the present paper, results of experimental and FEM analyses of pitting and stress distribution of gears are reported.

In the experimental measurements, an overload in terms of applied torque is used, in order to exert excessive stresses of gear and to produce pitting within a short time. In these accelerated endurance tests, the goal is to get a pitting of order of 4-8% in terms of relative size in undamaged gears under non-stationary conditions.

A FEM model is developed in order to simulate the same test rig considered in the pitting tests, including gear crowning. Numerical analyses estimate contact pressure and normal stress distribution on the gear teeth, which are the bases for diagnosis, root cause analysis and prognosis technologies based on vibration measurements of gear damage.

2. EXPERIMENTAL ANALYSIS OF GEAR PITTING

In this section, experimental activities performed by means of accelerated endurance tests in order to investigate the pitting phenomenon of gears are reported. The test rig used in the experimental activities is an open-loop configuration experiment designed for testing single gear pairs, with maximum torque of 200Nm and rotational frequency of 3000RPM. Two DC motors are present, one of them acts as a motor and the second has the role of electric brake (generator); the controller allows an internal electric energy recirculation.

The test rig considered allows single spur gear pairs with arbitrary centre distance and two angular misalignments to be tested. Two torque-meters measure the applied input and output torque, while four tangential rotating accelerometers measure the rotational vibration of the wheels and consequently the dynamic transmission error (DTE).

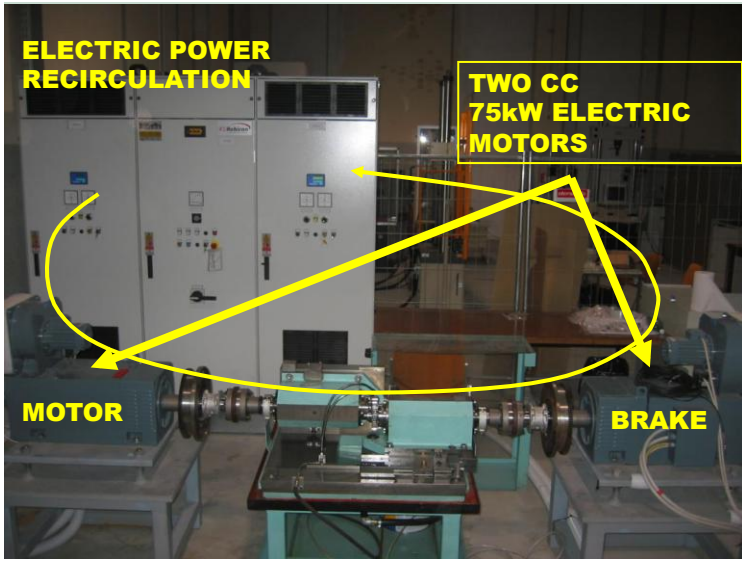

Figure 1. Test rig for the lab experiments.

Experimental Setup

The test bench considered is shown in Figure 1, two gears are mounted on shafts connected to two DC motors (engine + brake), these are highly balanced motors characterized by very low torque ripple.

Starting from the motor on the left of Figure 1, and moving to the right, one finds: i) a flywheel; ii) an elastic joint (Falk Steelflex T10" model 1050T); iii) a torque-meter; iv) an hollow super-stiff shaft mounted on two roller bearings, where the bearings are connected on a very stiff foundation.

The experimental setup consists mainly of three parts, as shown in Figure 2: i) control panel; ii) test bench gear; iii) data acquisition system.

The main features of the engine test stands are the following: maximum power 75KW, maximum speed 2880RPM. The motor M2 is used to rotate the pinion, while the motor M1 is used to provide the load torque to the wheel and therefore works as a brake. The control and regulation of the two motors can be done by acting on two parameters: revolutions per minute (RPM), current (A). The gear vibration is measured by tangential accelerometers.

The test bench is a gear system that can simulate and monitor the dynamic behaviour of gear pairs. The structure is constituted by two hollow shafts supported by two casings on which flanges are connected through screws. The possibility to mount the wheels on the shafts individually simulating the operation of a reduction gear represents a great advantage compared to the case in which it has to handle gearbox. In this way, it can be continuously monitored by mounted accelerometers. The test bench has a system of self-lubricating drop and the distance between the two gears can be adjusted via a micrometric screw.

A specific activity was carried out in order to design a special gear pair undergoing to a fast pitting phenomena with maximum available torque (DC engines) of 200Nm, where at the same time the bending failures must be avoided. This was reached by introducing a large amount of crowning along the face width. The goal was to obtain a gear pair so that the pitting arises within 60 hours. Accurate data on the gear material and surface finishing are needed for a proper estimate of the pitting phenomenon.

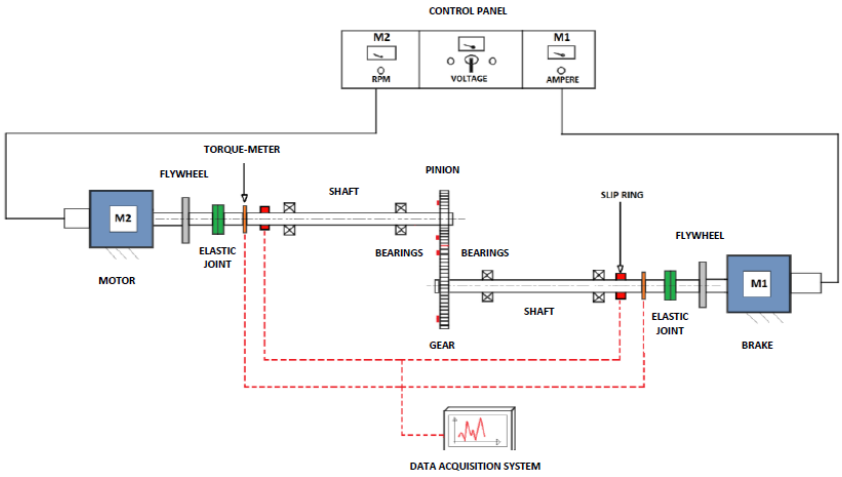

Figure 2. Scheme of the test rig.

Amplitude-Frequency Curves

In the present section, the first experiments performed on the test rig are described. The goal is to obtain amplitude-frequency diagrams in order to find out the main resonances of the gear transmission system by varying the excitation frequency, i.e., the mesh frequency.

Considering the reference load of the pinion equal to 130Nm, four tests were carried out at different vibration levels, i.e., percentual nominal loads.

For each load value, the interval of acquisition was 5s, from 100RPM to 1500RPM, with frequency step between two acquisitions equal to 20RPM. Filters were set as follows: i) moving average filter; ii) automatic cut-off frequency (accordingly to mesh frequency); iii) high pass filter at 50Hz.

Figure 3 shows the values of the RMS amplitude [g] obtained by varying the rotational frequency n [RPM] at the pinion for the four different external loads. In all the cases, the highest peak is found at 1200RPM, corresponding to 640Hz, which is the natural frequency of resonance of the system. Moreover, the resonance peak has an amplitude equal to 1.7g (100% of nominal load).

Durability and Pitting Tests

After performing tests for measuring the transmission error, pitting tests are carried out. These durability tests are made at the nominal load (130Nm), far from the resonance: the chosen frequency is 840RPM, which corresponds to the minimum value of RMS amplitude of 0.2g. The signals were collected by two tri-axial accelerometers on pinion and gear shaft supports respectively, and by two uni-axial accelerometers on motor side and on brake side.

After a 4 hours test performed at external torque 130Nm, speed 840RPM and external temperature 20°C, a visible pitting phenomenon arises, with the presence of two craters on the side of two adjacent teeth of the pinion, together with several smaller pits.

In particular, the pitting phenomenon is present in four different teeth (4,8,9,12), where for each pitted tooth the pitting size is estimated as a percentual of the total flank area 1.42cm^2 (the pitting sizes are 3.3%, 4.4%, 2%, 1.1%, respectively), see Figures 4-8.

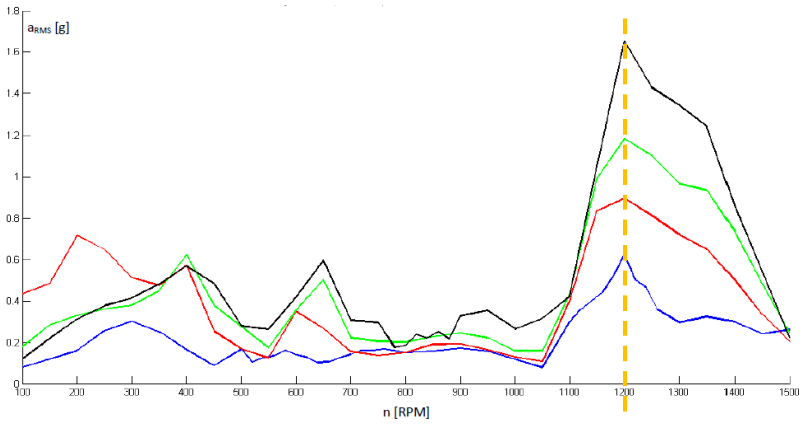

Figure 3. Amplitude-frequency curves for different external loads. 100-1500RPM. — 15% of the nominal load (20Nm); — 50% of the nominal load (65Nm); — 80% of the nominal load (105Nm); — 100% of the nominal load (130Nm).

Figure 4. Numbering of the pitted teeth (4,8,9,12) of the pinion. Tooth 1 as reference.

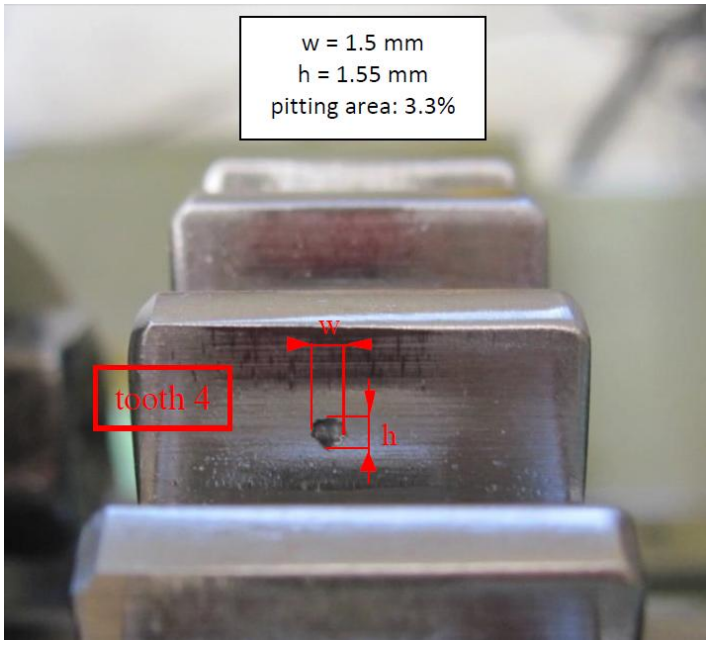

Figure 5. Pitting on tooth 4 of the pinion.

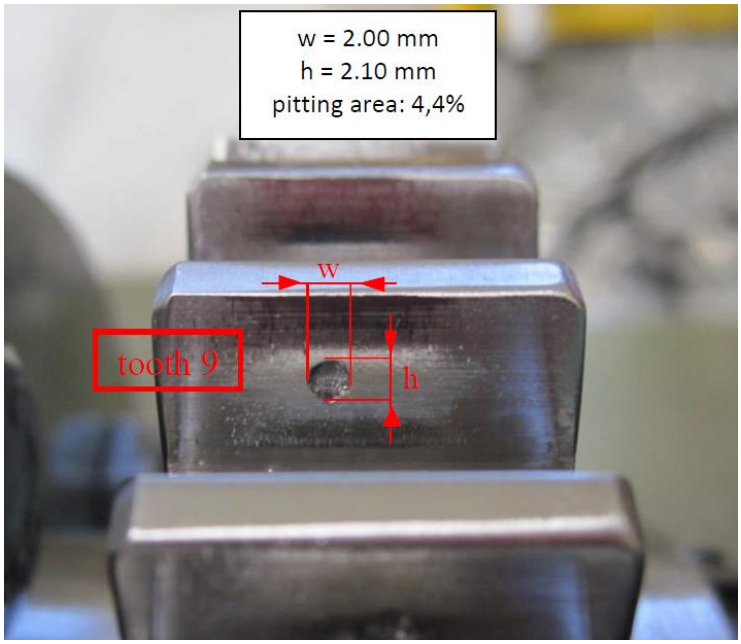

Figure 6. Pitting on tooth 9 of the pinion.

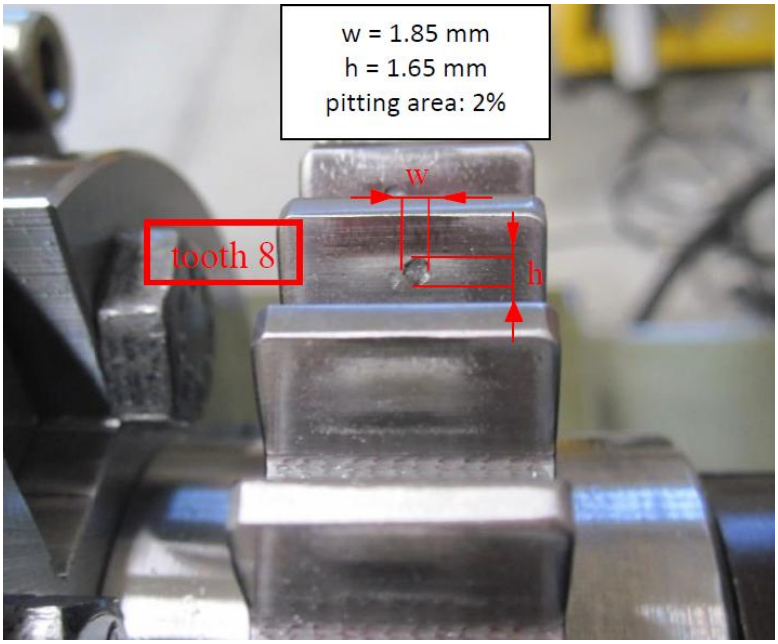

Figure 7. Pitting on tooth 8 of the pinion.

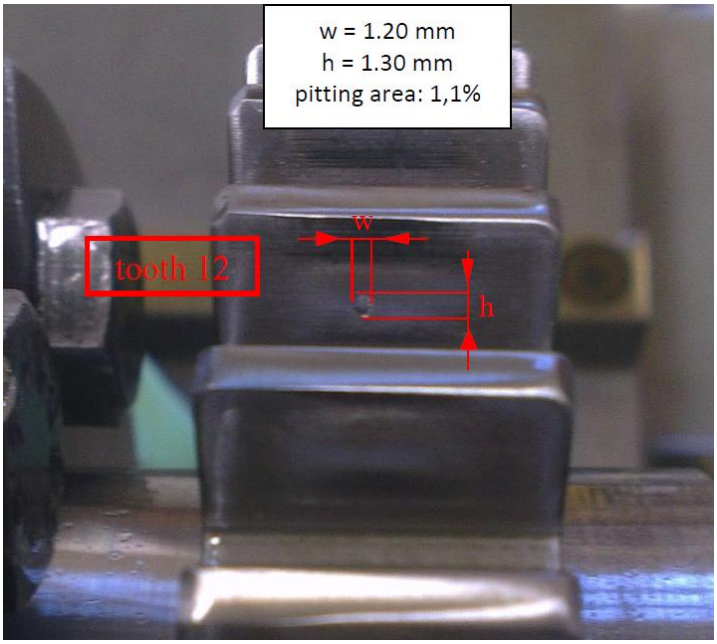

Figure 8. Pitting on tooth 12 of the pinion.

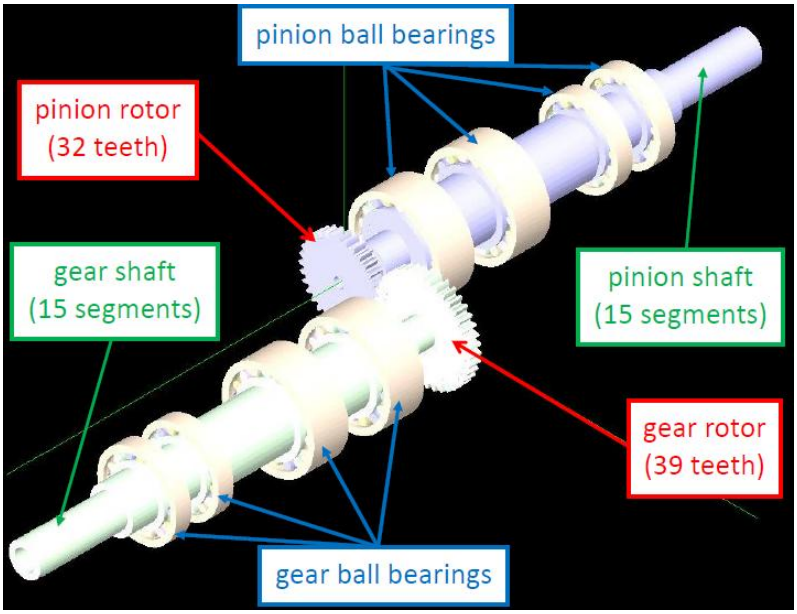

Figure 9. FEM modelling of the mechanical system (pinion, gear, shafts, bearings).

3. NUMERICAL ANALYSIS OF GEAR STRESS

In this section, results of finite element analyses performed in order to obtain the gear stress distribution and to validate the experimental stress-vibration correlations are reported.

The FEM modelling of the test rig is carried out using the numerical software Calyx® (Transmission3D): the multi-body finite element model is build up, the stresses and strains of the different elements of the mechanical system are investigated.

The FEM modelling of the overall mechanical system (pinion, gear, shafts, bearings) is shown in Figure 9.

The mechanical system is composed by:

- pinion rotor (sun: 32 teeth, shaft: 15 segments, bearing inner race: 6 sectors);
- gear rotor (sun: 39 teeth, shaft: 15 segments, bearing inner race: 6 sectors);
- ground (bearing outer race: 12 sectors);
- bearings (pinion: 2 sectors × 15 rollers + 4 sectors × 17 rollers, gear: 4 sectors × 17 rollers + 2 sectors × 15 rollers).

In the present dynamic analyses, the external torque is applied to the pinion, while the rotational frequency is applied to the gear; the displacement constrains (u,v,w) = 0 are imposed to the pinion; the displacement constrains (u,v,w) = 0 and the rotational constraints ($\theta x,\theta y,\theta z$) = 0 are imposed to the gear.

The dynamic factors and RMS accelerations obtained by means of a 2-dof dynamic model previously developed are given in Table 1; these last results are used in the dynamic FEM simulations in order to obtain numerical stress-vibration correlations.

In particular it must be underlined that test A (with n_1=0RPM) denotes a static analysis, tests B-E (with n_1=800-1325RPM) represent dynamic analyses.

In the following, the maximum normal stress and contact pressure on the contact tooth of the pinion vs. vibration amplitude for the different cases of Table 1 are investigated.

Maximum Normal Stress vs. Vibration Amplitude

In Figure 10, the behaviour of the maximum normal stress σ_{max} at the base of the contact tooth of the pinion rotor vs. the vibration amplitude a_{RMS} at the initial contact time obtained by FEM analyses is reported.

The input rotor is the pinion (contact tooth 25), the output rotor is the gear (contact tooth 9).

The external torques T[Nm] of Table 1 are imposed to the pinion. The corresponding values of maximum normal stress are reported in Table 2.

From Figure 10, it can be observed a linear behaviour of the maximum normal stress for all the vibration amplitudes considered.

Table 1. Dynamic factors and RMS accelerations.

Test	**n_1[RPM]**	**a_{RMS}[g]**	**T[Nm]**	**$f_d=T/T_n$**
A	0	0	130.0	1.00
B	800	0.15	161.2	1.24
C	985	0.33	194.0	1.49
D	1200	1.73	455.5	3.50
E	1325	0.73	256.8	1.97

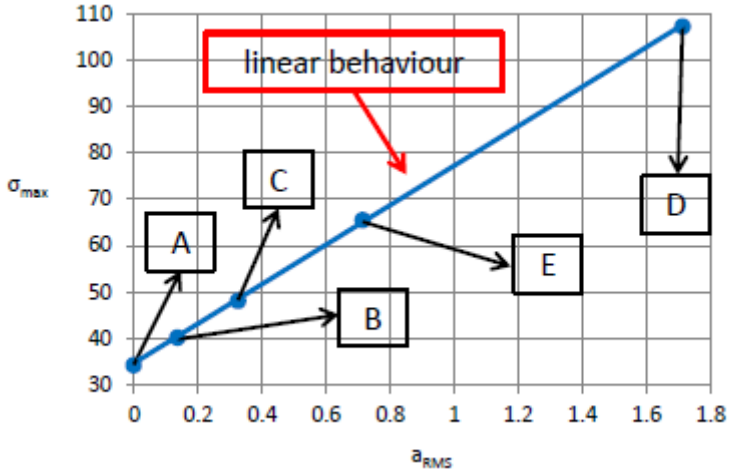

Figure 10. Maximum normal stress σ_{max} at the base of the contact tooth of the pinion rotor vs. vibration amplitude a_{RMS}. FEM analyses.

Maximum Contact Pressure vs. Vibration Amplitude

In Figure 11, the maximum contact pressure p_{max} on the contact tooth of the pinion rotor vs. the vibration amplitude a_{RMS} at the initial contact time obtained by FEM analyses is reported.

The input rotor is the pinion (contact tooth 25), the output rotor is the gear (contact tooth 9).

The imposed lead crown surface modification along the face width of the teeth gives a semi-elliptical Hertzian distribution of the contact normal pressure.

The different external torques T reported in Table 1 are imposed to the pinion. The values of maximum contact pressure are reported in Table 3.

From Figure 11, it can be observed an initial nonlinear behaviour of the maximum contact pressure (for a_{RMS}=0-0.5g, tests A-B-C), which becomes quasi-linear by increasing the vibration amplitude (for a_{RMS}=0.5-1.8g, tests E-D).

Table 2. Maximum normal stress vs. Vibration amplitude.

Test	a_{RMS}[g]	σ_{max}[N/mm^2]
A	0	33.2
B	0.15	40.5
C	0.33	48.2
D	1.73	106.4
E	0.73	62.6

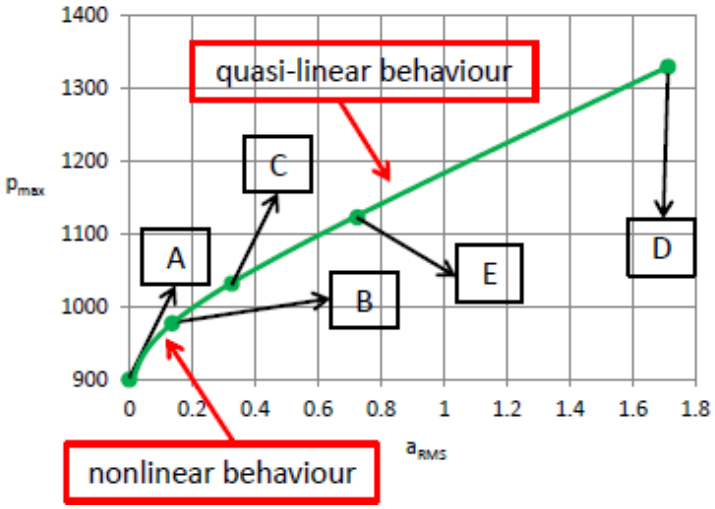

Figure 11. Maximum contact pressure p_{max} on the contact tooth of the pinion rotor vs. vibration amplitude a_{RMS}. FEM analyses.

4. CONCLUSIONS

In this paper, the pitting phenomenon and stress distribution of gears are considered.

Pitting durability experimental tests are made at 130Nm of nominal load, 840RPM of rotational frequency and 0.2g of RMS amplitude.

After a 4 hour test at an external temperature of 20°C, a visible pitting phenomenon is present in four different teeth (4,8,9,12) of the pinion, where for each pitted tooth the pitting size is estimated as a percentual of the total flank area 1.42cm^2, with pitting sizes 3.3%, 4.4%, 2%, 1.1%, respectively.

Numerical FEM analyses are performed in order to investigate gear contact pressure and normal stress distribution.

The maximum normal stress at the base of the contact tooth of the pinion at the initial time presents a linear behaviour for all the vibration amplitude values.

The maximum contact pressure on the contact tooth of the pinion at the initial time gives an initial nonlinear behaviour, which becomes quasi-linear by increasing the vibration amplitude.

Table 3. Maximum contact pressure vs. vibration amplitude.

Test	a_{RMS}[g]	p_{max}[N/mm^2]
A	0	904.7
B	0.15	972.4
C	0.33	1023.2
D	1.73	1329.7
E	0.73	1108.6

REFERENCES

[1] Fukumasu NK, Machado GAA, Souza RM, and Machado IF, 2016. "Stress Analysis to Improve Pitting Resistance in Gear Teeth", *Proceedings of the 3rd CIRP Conference on Surface Integrity*, **45**, pp. 255-258.

[2] Faggioni M, Samani FS, Bertacchi G, and Pellicano F, 2011. "Dynamic optimization of spur gears", *Mechanism and Machine Theory*, **46**, pp. 544-557.

[3] Bonori G, Barbieri M, and Pellicano F, 2008. "Optimum profile modifications of spur gears by means of genetic algorithms", *Journal of Sound and Vibration*, **313**, pp. 603-616.

[4] Barbieri M, Bonori G, and Pellicano F, 2012. "Corrigendum to: Optimum profile modifications of spur gears by means of genetic algorithms", *Journal of Sound and Vibration*, **331**, pp. 4825-4829.

[5] Choy FK, Polyshchuk V, Zakrajsek JJ, Handschuh RF, and Townsend DP, 1996. "Analysis of the effects of surface pitting and wear on the vibration of a gear transmission system", *Tribology International*, **29**, pp. 71-83.

[6] Barbieri M, Zippo A, and Pellicano F, 2014. "Adaptive grid-size finite element modelling of helical gear pairs", *Mechanism and Machine Theory*, **82**, pp. 17-32.

[7] Masoumi A, Pellicano F, Samani FS, and Barbieri M, 2015. "Symmetry breaking and chaos-induced imbalance in planetary gears", *Nonlinear Dynamics*, **80**, pp. 561-582.

[8] Del Rincon F, Viadero F, Iglesias M, De-Juan A, Garcia P, and Sancibrian R, 2012. "Effect of cracks and pitting defects on gear meshing", *Proceedings of the IMechE Part C: Journal of Mechanical Engineering Science*, **226**, pp. 2805-2815.

[9] Gelman L, Chandra NH, Kurosz R, Pellicano F, Barbieri M, and Zippo A, 2016. "Novel spectral kurtosis technology for adaptive vibration condition monitoring of multi-stage gearboxes", *Non-Destructive Testing and Condition Monitoring*, **58**, pp. 409-416.

[10] Barbieri M, Lubrecht AA, and Pellicano F, 2013. "Behavior of lubricant fluid film in gears under dynamic conditions", *Tribology International*, **62**, pp. 37-48.